

Journal Pre-proof



Functionalized Biochar for the Removal of Poly- and Perfluoroalkyl Substances in Aqueous Media

Sepideh Nasrollahpour, Rama Pulicharla, Satinder Kaur Brar

PII: S2589-0042(25)00373-6

DOI: <https://doi.org/10.1016/j.isci.2025.112113>

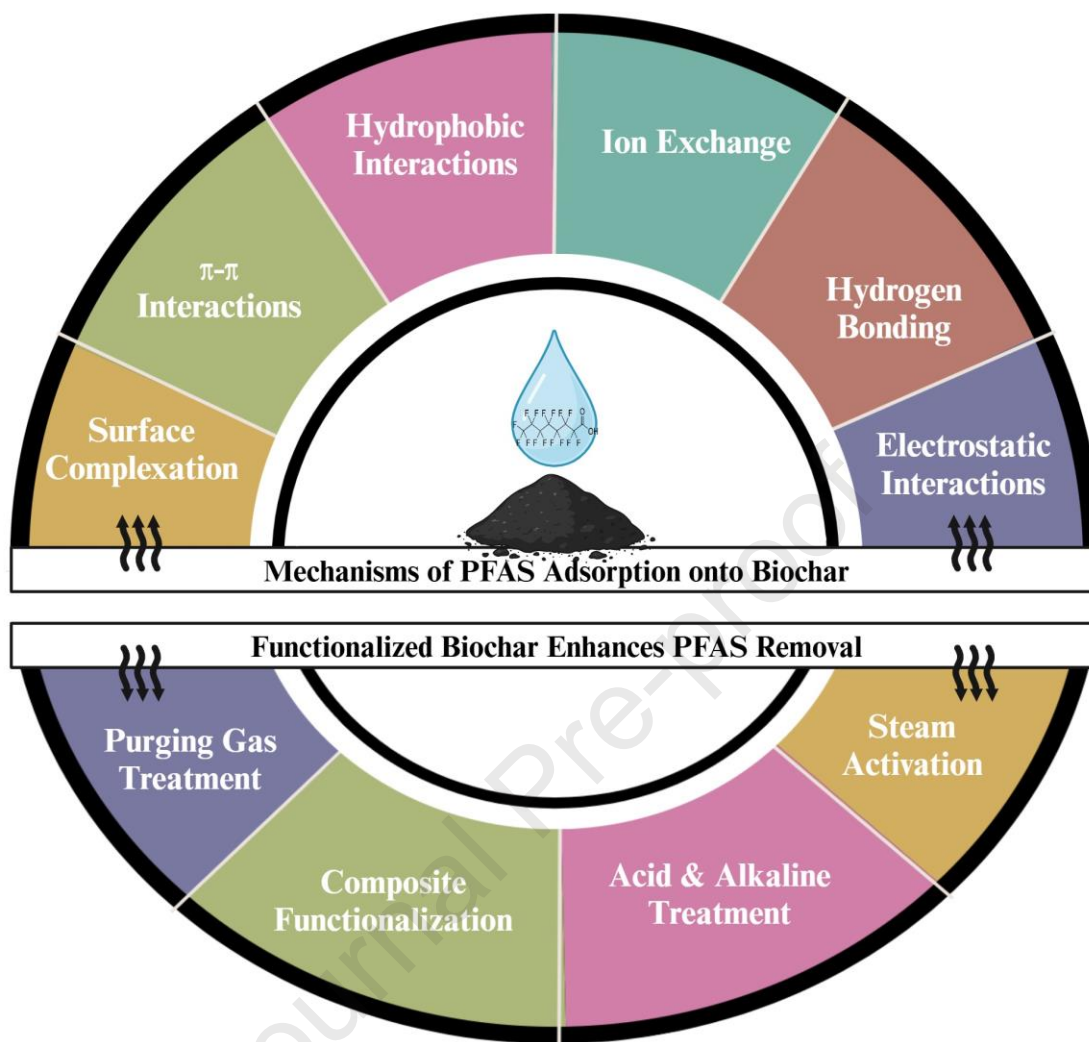
Reference: ISCI 112113

To appear in: *ISCIENCE*

Please cite this article as: Nasrollahpour, S., Pulicharla, R., Brar, S.K., Functionalized Biochar for the Removal of Poly- and Perfluoroalkyl Substances in Aqueous Media, *ISCIENCE* (2025), doi: <https://doi.org/10.1016/j.isci.2025.112113>.

This is a PDF file of an article that has undergone enhancements after acceptance, such as the addition of a cover page and metadata, and formatting for readability, but it is not yet the definitive version of record. This version will undergo additional copyediting, typesetting and review before it is published in its final form, but we are providing this version to give early visibility of the article. Please note that, during the production process, errors may be discovered which could affect the content, and all legal disclaimers that apply to the journal pertain.

© 2025 The Author(s). Published by Elsevier Inc.



Functionalized Biochar for the Removal of Poly- and Perfluoroalkyl Substances in Aqueous Media

Sepideh Nasrollahpour¹, Rama Pulicharla¹, Satinder Kaur Brar^{1,*}

¹Department of Civil Engineering, Lassonde School of Engineering, York University, Toronto, Canada.

*Corresponding author: satinderbrar@lassonde.yorku.ca

Abstract

Biochar has gained attention as a promising adsorbent for removing various environmental pollutants due to its availability, cost-effectiveness, eco-friendly nature, and high adsorption capacity. This review focuses on using biochar to remove poly- and perfluoroalkyl substances (PFAS), emerging contaminants that pose significant environmental and health risks due to their toxicity, persistence, and bioaccumulation potential. The classification of biochar and using pristine and functionalized biochar for pollutant removal are addressed, along with an overview of the various functionalization techniques employed to enhance biochar's adsorption capacity. Different factors influencing the removal of poly- and perfluoroalkyl substances (PFAS), such as pH, the molecular chain length of PFAS, and biochar characteristics like pyrolysis temperature, particle size, and dosage, are investigated. Long-chain PFAS, such as perfluoro octane sulfonate (PFOS) and perfluorooctanoic acid (PFOA), are more effectively adsorbed than short-chain PFAS, with competitive sorption effects observed in mixed-solution environments. A decrease in pH, smaller biochar particle sizes, and optimized pyrolysis temperatures have been found to enhance biochar's sorption capacity. Furthermore, biochar demonstrates higher efficiency in single-solution systems compared to mixed solutions when removing PFAS.

Keywords: Biochar, Poly- and Perfluoroalkyl Substances (PFAS), Functionalization, Removal.

Introduction

Biochar is a carbon-rich material produced through the pyrolysis of biomass in the absence of oxygen. Its unique physicochemical properties, such as high surface area, porosity, and chemical stability, make it an appealing material for a wide range of applications, including agriculture, energy production, and environmental remediation. Derived from organic waste materials such as agricultural residues, wood chips, and sewage sludge, biochar contributes to sustainable waste management and carbon sequestration. Its low cost and high availability make it an attractive alternative to conventional adsorbents like activated carbon in water and soil treatment ¹.

In wastewater treatment, biochar has demonstrated considerable potential through mechanisms such as adsorption, catalysis, and ion exchange. However, the adsorption capacity of pristine biochar is often limited by its low surface area and susceptibility to abiotic and biotic degradation. To overcome these limitations, researchers have focused on the functionalization of biochar. Functionalization processes, such as impregnation with metal oxides, steam activation, and acid-base treatments, are designed to enhance biochar surface area, introduce more active sites, and improve its mechanical properties. Functionalized biochar, with its increased adsorption capacity,

39 has shown great promise in efficiently removing organic and inorganic pollutants from aqueous
40 solutions ².

41 One of the latest environmental challenges is the removal of perfluoroalkyl and polyfluoroalkyl
42 substances (PFAS) from contaminated water. PFAS are synthetic chemicals used in various
43 industries, including firefighting foams, textiles, and food packaging. Due to their strong carbon-
44 fluorine (C-F) bonds, PFAS are chemically stable and resistant to environmental degradation,
45 leading to their accumulation in water, soil, and living organisms. Long-chain PFAS compounds,
46 such as perfluorooctanoic acid (PFOA) and perfluoro octane sulfonate (PFOS), are particularly
47 harmful, having been linked to health issues such as elevated cholesterol, cancer, and
48 developmental effects in children ³⁴.

49 The persistence and bioaccumulative nature of PFAS make them difficult to remove from the
50 environment, posing a significant risk to human health. In the United States alone, As of May 2024,
51 6189 sites have been identified as PFAS-contaminated, affecting public and private water supplies.
52 In Canada, more than 100 federal sites are confirmed or suspected to be contaminated with PFAS.
53 These sites are spread across all provinces and territories, with the majority linked to the past or
54 ongoing use of aqueous film-forming foam (AFFF) at airports and military facilities. The
55 hydrophobic nature and high Log K_{ow} values of PFAS, especially the long-chain compounds, make
56 them poorly soluble in water and prone to accumulate in natural water bodies. Regulatory agencies,
57 such as the U.S. Environmental Protection Agency (EPA), have set a 70 ppt limit for PFOA and
58 PFOS in drinking water, but achieving these limits through traditional remediation methods is
59 challenging ^{56,7}.

60 Various techniques, including ion exchange, advanced oxidation, coagulation, graphene and
61 membrane filtration, have been explored for PFAS remediation. However, these methods often
62 suffer from drawbacks such as high costs, low efficiency, and the production of secondary
63 pollutants⁸⁹ Among the solutions, biochar, particularly functionalized biochar, has shown great
64 promise for PFAS removal due to its low cost, wide availability, and environmentally friendly
65 nature. The functionalization of biochar enhances its ability to adsorb PFAS through mechanisms
66 such as hydrophobic interactions, electrostatic attraction, and, in certain cases, π - π bonding when
67 aromatic systems are present ¹⁰¹¹¹²¹³¹⁴. Recent advancements in functionalization techniques have
68 significantly improved biochar performance in PFAS removal by increasing its surface area and
69 functional group density¹⁵¹⁶.

70 This review explores the potential of biochar, especially functionalized biochar, as a sustainable
71 material for PFAS removal from aqueous environments. It offers a detailed synthesis of biochar
72 characterization methodologies (physical and chemical), pollutant removal mechanisms, and
73 limitations of conventional PFAS treatments. By examining the role of pristine and functionalized
74 biochars, functionalization techniques, and key variables affecting PFAS removal (e.g., pH, PFAS
75 chain length, pyrolysis conditions, and particle size), this review identifies pathways to optimize
76 biochar performance. This review focuses on integrating these insights to bridge gaps in knowledge
77 and advance biochar-based PFAS remediation.

78 **Biochar characterization methodologies**

79 Recent research highlights the importance of comprehensive characterization techniques for
80 biochar to identify its agricultural and environmental benefits and differentiate it from other organic
81 materials with similar properties. The diverse characteristics of biochar, include its stability,
82 specific surface area, functional groups on its surface, structure, and elemental composition, make
83 it difficult to select the most appropriate characterization methods. The characteristics of biochar
84 can be categorized into four main groups, including chemical, physical, structural, and thermal
85 stability properties. Various techniques are reported in literature, including Cation Exchange
86 Capacity (CEC), Scanning Electron Microscopy (SEM), Energy-dispersive X-ray spectroscopy
87 (EDX or EDS), X-Ray Diffraction (XRD), Zeta potential, Fourier Transform Infrared Spectrometer
88 (FTIR), X-Ray photoelectron spectrometry (XPS), Brunauer Emmett Teller (BET), Differential
89 scanning calorimetry (DSC), Ash and moisture, Thermo Gravimetric Analysis (TGA), and Raman
90 spectroscopy¹⁷¹⁸¹⁹.

91 The frequency of using various techniques for biochar characterization in PFAS elimination
92 investigations is displayed in **Figure 1**. The most used techniques in biochar literature are FTIR,
93 SEM/TEM, and BET, respectively.

94 95 96 **Physical characteristics**

97 The physical attributes of biochar, such as particle size distribution, bulk density, pore size and
98 volume distribution, and specific surface area (SSA), are influenced by factors such as pyrolysis
99 conditions (temperature, residence time) and the presence of oxygen-containing media like air,
100 CO₂, or steam. These properties are key in determining biochar adsorption capacity.
101 Characterization techniques, particularly the BET method, are critical for assessing SSA and how
102 pyrolysis conditions modify biochar's structural features. Studies have demonstrated that higher
103 pyrolysis temperatures can increase both SSA and total pore volume. Moreover, post-treatment
104 processes like acid treatments enhance SSA by introducing inorganic materials on the biochar
105 surface, modifying the pore structure. Additionally, reduced pore sizes are observed alongside
106 increases in total pore volume, revealing a complex relationship between these factors²⁰²¹²².

107 **Chemical characteristics**

108 The chemical properties of biochar, including its surface functional groups, oxygen-to-carbon
109 (O/C) ratio, and CEC, are crucial in determining its effectiveness for PFAS removal. The O/C ratio,
110 often analyzed through EDX/EDS, directly correlates with the extent of carbonization. Lower O/C
111 ratios indicate higher aromaticity, which can enhance hydrophobic interactions with PFAS,
112 reducing surface polarity and improving adsorption capacity. CEC, representing the biochar's
113 ability to exchange cations, enhances PFAS adsorption by providing ionic exchange sites. Higher
114 CEC biochars are more effective, particularly for cationic or zwitterionic PFAS, due to increased
115 electrostatic interactions. Environmental factors like competing ions and pH further influence this
116 property²³.

117 Surface functional groups, such as carboxyl and hydroxyl groups, identified via XPS and FTIR, are
118 one of the most critical properties for PFAS removal. These groups facilitate key interactions—

119 such as electrostatic attractions and hydrogen bonding—with PFAS molecules. FTIR analysis can
120 detect changes in these functional groups before and after adsorption, providing insights into the
121 mechanisms at play during the removal process ²⁴.

122 The point of zero charge (PZC) of biochar is another critical factor, as it dictates the surface charge
123 under different pH conditions. When the PZC is lower than the solution pH, the biochar surface
124 becomes negatively charged, promoting the adsorption of cationic PFAS or PFAS molecules in
125 acidic environments ²⁵.

126 **Surface morphology**

127 Surface morphology analysis via SEM/TEM offers critical insights into the pore structure and
128 surface defects of biochar, both pre- and post-treatment. High-resolution imaging can reveal
129 porosity alterations associated with PFAS adsorption, providing essential data on biochar reactive
130 sites. Raman spectroscopy is pivotal for assessing structural defects (D band) and graphitization (G
131 band), with the ID/IG ratio serving as a key metric for disorder. A higher ID/IG ratio signifies more
132 defective sites, enhancing PFAS adsorption. Additionally, XRD can identify crystalline versus
133 amorphous phases, offering insights into the stability of functionalized biochar, particularly in
134 metal oxide-modified composites critical for PFAS removal efficiency ²⁶.

135 **Stability characteristic of biochar**

136 TGA is crucial for evaluating biochar's thermal stability, revealing degradation profiles tied to its
137 structural composition. TGA differentiates distinct thermal decomposition stages: dehydration
138 (below 300°C), breakdown of labile components (300-400°C), and the gradual degradation of
139 recalcitrant carbon fractions at higher temperatures. For instance, a study on maple leaf-derived
140 biochar reported a 10% weight loss due to moisture evaporation and volatile release below 300°C,
141 followed by a 45% loss between 300-400°C, attributed to cellulose and hemicellulose degradation,
142 with minor weight loss above 400°C, corresponding to lignin and stable carbon forms. The steep
143 weight reduction between 300-400°C highlights biochar's susceptibility to thermal degradation in
144 this temperature range, providing insights into its recalcitrance and potential long-term
145 environmental stability ²⁷.

146 **Biochar's function in removal of pollutants**

147 Biochar removes pollutants through a combination of adsorption, ion exchange, complexation, and
148 precipitation mechanisms. These processes are governed by the physicochemical properties of
149 biochar, which depend on its feedstock and pyrolysis conditions.

150 **Adsorption**

151 The high surface area and porous structure of biochar enable it to physically adsorb a wide range
152 of contaminants. Organic pollutants, such as polycyclic aromatic hydrocarbons (PAHs) and
153 pesticides, are trapped within its micropores through van der Waals forces. Chemisorption,
154 involving covalent or hydrogen bonding, occurs when pollutant molecules interact with functional
155 groups such as hydroxyl (-OH), carboxyl (-COOH), and amine (-NH₂) on the biochar surface.
156 These groups enhance the binding of inorganic pollutants, including heavy metals like lead (Pb)
157 and cadmium (Cd). Adsorption efficiency is influenced by pH, ionic strength, temperature, and the
158 presence of competing contaminants. For instance, acidic conditions promote the adsorption of

159 cationic heavy metals by increasing electrostatic attraction to negatively charged biochar surfaces
160 ²⁸.

161

162 **Ion Exchange**

163 Ion exchange processes allow biochar to replace its surface ions (e.g., H⁺, Na⁺, K⁺) with pollutant
164 ions. This mechanism is particularly effective for the removal of cationic species such as
165 ammonium (NH⁴⁺), zinc (Zn²⁺), and copper (Cu²⁺). Biochar derived from nutrient-rich feedstocks,
166 such as animal manure, exhibits a higher cation exchange capacity (CEC) due to its abundance of
167 negatively charged functional groups and mineral constituents. The effectiveness of ion exchange
168 depends on environmental factors such as competing ions and solution pH, which influence the
169 surface charge and exchangeable ion availability of biochar ²⁹.

170 **Complexation**

171 Functional groups on the surface of biochar interact with pollutants, forming stable complexes that
172 immobilize contaminants. For example, carboxyl and phenolic groups bind with metals like
173 chromium (Cr) and mercury (Hg) to form chelated structures, reducing their solubility and mobility.
174 This mechanism is particularly relevant in water treatment and soil remediation, where the
175 immobilization of toxic elements is essential for environmental and public health ³⁰.

176 **Precipitation**

177 Mineral components within biochar, such as calcium (Ca) and magnesium (Mg), promote the
178 precipitation of certain pollutants into insoluble compounds. For instance, phosphate ions in
179 wastewater can react with calcium to form hydroxyapatite, effectively removing phosphates
180 through mineral precipitation. Similarly, fluoride ions interact with magnesium to form stable
181 precipitates, mitigating their environmental impact ³¹.

182 Additionally, pollutant removal is not restricted to just one mechanism but can entail several
183 methods. This multi-functionality is an advantage of biochar, but it complicates identifying which
184 mechanisms are most effective under specific conditions. Future research should clarify these
185 mechanisms to better tailor biochar applications for different pollutants.

186 **A summary of PFAS treatment**

187 The persistence of PFAS in aquatic ecosystems, including surface and groundwater, is due to their
188 resistance to conventional treatment processes. Industrial waste, wastewater discharge, and biosolid
189 applications lead to the accumulation of PFAS in tap water because of their strong carbon-fluorine
190 (C–F) bonds, which make them difficult to remove ³².

191 Current strategies for PFAS removal include destructive techniques (e.g., thermal and
192 electrochemical treatments) and separation methods (e.g., adsorption and membrane filtration).
193 Destructive methods often result in incomplete degradation and harmful byproducts due to the
194 stability of PFAS, which limits their real-world applicability as the production of secondary
195 pollutants complicates the remediation process. Moreover, these methods frequently fail to achieve
196 complete mineralization of PFAS, leaving behind harmful intermediates that reduce their
197 effectiveness for large-scale water treatment applications. Separation methods, such as reverse
198 osmosis and nanofiltration, are effective but costly, energy-intensive, and generate concentrated
199 PFAS waste streams. Coagulation-flocculation serves as a pretreatment, but alone it is insufficient
200 for PFAS removal ³³.

201 Granular activated carbon (GAC) is widely used, but its efficiency drops significantly in the
202 presence of natural organic matter (NOM) and with short-chain PFAS. Studies report that GAC
203 cannot be effective in removing short-chain PFAS like PFBS in complex wastewater. Ion-exchange
204 resins, while effective, have high costs and may produce carcinogenic byproducts, such as
205 nitrosamines, during water treatment³⁴. This raises health and safety concerns, particularly when
206 these byproducts are not sufficiently addressed during treatment processes.

207 Biochar, particularly when functionalized with substances like iron oxides or through other
208 chemical processes, offers a promising alternative, achieving over 80% removal of long-chain
209 PFAS. Unlike GAC, biochar is renewable, making it a sustainable option for large-scale
210 applications. While challenges remain for short-chain PFAS, biochar's potential as a low-cost,
211 environmentally friendly solution continues to grow³⁵.

212 **Different pristine biochar for PFAS treatment**

213 Some studies have used biochar for PFAS removal due to its unique features, as illustrated in **figure**
214 **2** by the abundance of PFAS contaminants removed by biochar and the number of publications in
215 the field of PFAS removal using biochar. Guo et al. found that corn straw biochar could remove
216 PFOS through hydrophobic and electrostatic interactions, with a maximum adsorption capacity of
217 0.34 mmol/g in eight hours. Increasing the pyrolysis temperature above 400°C improved the
218 biochar's ability to remove PFOS by increasing hydrophobicity, fine-pore structures, and surface
219 area. However, the PFOS adsorption capability of biochar decreased as the pH of the solution rose.
220 PFOS adsorption on biochar was identified as an endothermic and spontaneous process, suggesting
221 the feasibility of biochar for treating wastewater under varying conditions³⁶.

222 Inyang and Dickenson investigated biochar derived from pinewood and hardwood for PFOA
223 removal. Their study identified hydrophobic interactions as the primary mechanism for adsorption,
224 with a maximum adsorption capacity of 0.099 mmol/g. However, the presence of dissolved organic
225 carbon (DOC) in wastewater led to competitive sorption, filling the biochar pores and limiting
226 PFOA uptake. This underscores the challenge posed by co-contaminants in real-world wastewater
227 matrices. Notably, biochar was less effective at removing shorter-chain PFAAs compared to
228 longer-chain counterparts like PFOS, consistent with the enhanced sorption potential for more
229 hydrophobic PFAS molecules³⁷. Waste wood from the timber industry was also used to make
230 biochar for the remediation of PFOA, PFBS, PFBA, and PFOS, and similar adsorption capabilities
231 were identified. Electrostatic attraction as well as hydrophobic interaction were implicated in the
232 adsorption process for PFAS. The study found that competitive sorption of PFASs happened during
233 the adsorption mechanism, decreasing the removal efficiency of PFASs and adding four
234 compounds to a solution decreased the effectiveness of PFOS removal by 32.8% to 57.9%
235 compared to a solution which contains a single PFAS substance. This dramatic decrease in
236 efficiency raises concerns about biochar's reliability in environments where multiple contaminants
237 coexist, which is typical in most real-world water treatment scenarios. Such findings suggest that
238 biochar practical application may require additional pre-treatment steps or post-treatment methods
239 to ensure the effective removal of all contaminants. Surface examination using FTIR revealed the
240 existence of diverse functional groups on the adsorbents, with some alterations in FTIR responses
241 revealing electronic interactions throughout sorption. The outcomes show that the adsorption

242 method is a promising strategy for controlling PFAS pollution in wastewater, and biochar has been
243 shown to be an efficient PFAS adsorbent ³⁸.

244 Chen et al. investigated biochar produced from maize straw and willow sawdust and found that
245 hydrophobic interactions were the primary mechanism for PFOS removal. Despite the negatively
246 charged surfaces of these biochars, which posed a challenge for PFOS adsorption, the study
247 reported maximum sorption capacities of 0.18 mmol/g and 0.33 mmol/g for willow sawdust and
248 maize straw biochar, respectively. The larger surface area of maize straw biochar (11.63 m²/g)
249 compared to willow sawdust biochar (7.21 m²/g) have contributed to its higher adsorption capacity.
250 However, other factors, such as pore size distribution and the presence of competing chemicals in
251 the water, also influence the effectiveness of PFAS removal ³⁹.

252 Overall, pristine biochar has proven to be efficient adsorbents for PFAS, particularly through
253 hydrophobic and electrostatic interactions. However, the variability in raw materials and the
254 influence of external factors such as pH, DOC, and competing contaminants limit their widespread
255 application without further optimization. The development of functionalization techniques could
256 enhance their adsorption capacity for PFAS. The word cloud in **Figure 3** illustrates the keywords
257 commonly used in articles discussing PFAS removal using biochar.

258

259 **Functionalized biochar for PFAS removal**

260 Functionalization of biochar can enhance its removal capabilities for PFASs by modifying its
261 surface chemistry, increasing its surface area, and introducing new functional groups. These
262 changes improve the biochar's affinity for PFAS through enhanced adsorption mechanisms, such
263 as electrostatic interactions, hydrophobic interactions, and improved sorption capacity. **Figure 4**
264 illustrates the functionalization approaches applied to biochar for PFAS remediation, where nearly
265 half of the studies involved pristine biochar, and the most commonly used functionalization agents
266 were KOH and ZVI. Additionally, Table S1 summarizes the experimental conditions and results
267 from these studies.

268

269 **Biochar functionalization by composites for PFAS removal**

270 In recent years, incorporating foreign components into biochar has become a technique for
271 producing hybrid composite materials with multiple functions. These composites offer novel
272 physicochemical features unavailable in the feedstock or pyrolyzed biomass. Tan et al. (2016)
273 classified biochar-based nanocomposites into groups: magnetized biochar, functional nanoparticle-
274 impregnated biochar composites, and nanometal oxide/hydroxide-biochar composites ⁴⁰.

275 **Magnetic biochar**

276 Magnetization of biochar involves incorporating magnetic materials, typically iron oxides (such as
277 Fe₃O₄), through methods like pyrolysis or co-precipitation. This enhancement allows for easy
278 separation of the biochar from water using magnets, reducing the need for additional filtration

279 processes. Magnetic biochar has gained significant attention for wastewater treatment due to its
280 high efficiency in adsorbing contaminants and its reusability ⁴¹.

281 Magnetic biochar has shown notable efficacy in the adsorption of PFAS. Hassan et al. demonstrated
282 that sugarcane bagasse, functionalized with Fe₂O₃ and subjected to low-temperature pyrolysis,
283 retained hydrophilic oxygen-containing groups, enhancing its PFOS adsorption capacity to 120.44
284 mg/g. Electrostatic interactions and chemisorption played a significant role in binding PFOS to the
285 biochar surface ⁴².

286 In another study, *Calotropis gigantea* fibres were pyrolyzed and magnetized with Fe₃O₄
287 nanoparticles. The resulting composite exhibited adsorption capacities of 204.7 mg/g for PFOA
288 and 195.5 mg/g for PFOS. These values were higher compared to non-magnetic biochar,
289 showcasing the enhanced affinity for PFAS removal ⁴³.

290 Magnetic biochar presents notable benefits, such as improved separation efficiency; however, its
291 practical application is not without challenges. The process of magnetic functionalization can
292 significantly raise production costs, potentially hindering its scalability for widespread use.
293 Additionally, the durability of magnetic biochar's adsorption efficiency in real-world conditions,
294 particularly in complex water systems with competing ions and contaminants, is still poorly studied.
295 Long-term research is needed to evaluate whether magnetic biochar can sustain its high adsorption
296 performance over repeated treatment cycles.

297 **Functional nanoparticle-impregnated biochar**

298 Functional nanoparticle-impregnated biochar composites have demonstrated efficiency in
299 removing PFAS. Nanoparticles such as nanoscale zero-valent iron (nZVI), graphene, carbon
300 nanotubes, and metal oxides like ZnS and Fe₃O₄, are incorporated into biochar to enhance its
301 adsorption and reactivity properties. For instance, nZVI-modified biochar can induce redox
302 reactions, helping to break down PFAS molecules while increasing the adsorption capacity. The
303 high surface area and reactivity of nanoparticles can compensate for the potential pore-blocking
304 effect during functionalization, allowing superior pollutant removal efficiency ⁴⁴.

305 Studies reveal that biochar impregnated with nZVI has shown enhanced performance for
306 removing perfluorooctanoic acid (PFOA). In one study, a composite biochar created using nZVI
307 via carbothermal reduction demonstrated a remarkable 99.9% PFOA removal rate at high
308 temperatures within six hours. Furthermore, a defluorination rate of 63.2% was achieved after
309 prolonged treatment. This was largely attributed to the prevention of nZVI particle agglomeration
310 during the carbothermal process, thus increasing the exposure of reactive sites for PFAS
311 degradation. Such composites also exhibit electron transfer capabilities, contributing to the
312 breakdown of PFAS via mechanisms like Kolbe decarboxylation, which results in shorter-chain,
313 less toxic perfluorinated compounds.

314 Additionally, studies on other nanoparticles, such as graphene oxide and chitosan-modified
315 biochar, show that these materials can enhance PFAS removal through mechanisms like
316 electrostatic interactions and hydrophobic adsorption. The versatility of biochar composites
317 means that their modification with nanoparticles can be tailored to target specific PFAS
318 compounds or mixtures ⁴⁵.

319 Despite the promising results, nanoparticle-impregnated biochar may introduce environmental
320 and operational concerns. The release of nanoparticles into treated water can pose additional
321 environmental risks, and the potential health impacts of such nanoparticles are not well studied.
322 Moreover, the synthesis of these composite materials often requires complex and costly
323 procedures, which may not be sustainable for widespread implementation.

324 **Composites of nanometal oxide/hydroxide and biochar**

325 Nanometal oxide-biochar composites have significant potential for PFAS removal due to their
326 synergistic physicochemical properties. The integration of nanometal oxides, such as MnO_2 , Fe_3O_4 ,
327 and Al_2O_3 , with biochar enhances adsorption by providing additional active sites and promoting
328 mechanisms such as surface complexation, electrostatic interactions, and hydrophobic attraction.
329 Biochar's porous structure facilitates the adsorption of hydrophobic PFAS chains, while the
330 nanometal oxides contribute positively charged functional groups that attract the negatively
331 charged PFAS molecules ⁴⁶.

332 In one study, researchers produced Nano- MnO_2 -biochar composites (NMBCs) by reducing
333 potassium permanganate in a biochar suspension with ethanol. The maximum Cu(II) sorption
334 capacity of NMBCs reached 142.02 mg/g, significantly higher than that of biochar (26.88 mg/g)
335 and nano- MnO_2 alone (93.91 mg/g) ⁴⁷. Such enhancements indicate that nanometal oxide-biochar
336 composites have strong potential for PFAS removal, though direct studies specifically targeting
337 PFAS are still limited. Further research should prioritize exploring their effectiveness in PFAS
338 remediation.

339 **Biochar Functionalization by Steam**

340 Steam activation is a process that enhances the physical properties of biochar, such as its surface
341 area, pore volume, and polarity, thereby improving its capacity to adsorb pollutants from water.
342 Following the first pyrolysis stage, steam is introduced to the reactor for 0.5 to 3 hours, which
343 expands inner pores and removes trapped volatile compounds like aldehydes and acids. This results
344 in a higher micropore volume and increased oxygen-containing functional groups, making steam-
345 activated biochar more effective in removing contaminants ⁴⁸.

346 In a study, Seven different biochars were evaluated for their ability to remove perfluoroalkyl acids
347 (PFAA) from field waters. Steam-activated pinewood biochar, produced at 700°C , showed
348 significantly higher adsorption of PFOA with a K_d value of 49 L/g, compared to other biochars.
349 This enhanced performance is due to its greater pore volume and carbon content. Moreover, steam-
350 activated biochar have faster sorption kinetics for PFAS like PFOA and PFBA, indicating that the
351 activation process may be optimizing the biochar for PFAS-specific sorption mechanisms ³⁷.
352 Despite these promising results, it is important to note that the high energy requirements for steam
353 activation could be a limiting factor for large-scale applications, making it less cost-effective
354 compared to other functionalization methods.

355 **Functionalization by purging gas**

356 This technique is employed during biomass pyrolysis or biochar activation, where specific gases
357 are introduced to modify the biochar's properties. This process can enhance the microporous

358 structure, increase the surface area, and alter the pore morphology and chemical composition of
359 biochar, thereby improving its effectiveness in various applications ⁴⁹.

360 Gases such as carbon dioxide (CO₂) and ammonia (NH₃) have been utilized at varying temperatures
361 for biochar activation and modification. The choice of gas and its flow rate can significantly
362 influence the characteristics of the biochar. For instance, CO₂-assisted activation can increase the
363 biochar's surface area and develop a microporous structure, making it particularly beneficial for
364 applications such as water and wastewater treatment. Additionally, the incorporation of alkali
365 metals during this process can enhance cation exchange capacity, further improving biochar's
366 functionality ⁵⁰.

367 While gas purging methods have been explored for the removal of heavy metals—such as the use
368 of nitrogen or CO₂ to remove lead (II), cadmium (II), copper (II), and nickel (II)—their application
369 in PFAS removal has been less explored and requires further investigation ⁵¹.

370 **Acid and Alkaline treatment**

371 These treatments influence the biochar surface area, pore structure, and chemical functionality,
372 improving both physical adsorption and chemical interaction with pollutants. Acid treatments,
373 using agents like hydrochloric, nitric, citric, or phosphoric acid, are commonly applied to remove
374 inorganic ash, increase surface oxygenated functional groups, and improve porosity. This enhances
375 biochar's capacity for adsorbing organic compounds and metals from contaminated media ⁵².
376 Alkaline treatments, typically involving sodium hydroxide (NaOH) or potassium hydroxide
377 (KOH), create significant structural changes by increasing surface area, pore volume, and
378 hydrophobicity. This modification is particularly effective for hydrophobic contaminants like
379 PFAS, as it enhances the biochar affinity for these compounds ⁵³.

380 For instance, coconut shell-derived biochar treated with molten KOH at 900°C produced a series
381 of hierarchically microporous biochars (HMBs), with surface areas ranging from 462 to 1322 m²/g.
382 The biochar's hydrophobicity also increased, making it more effective at adsorbing PFOA. The
383 most efficient biochar (HMB900-2.4) showed a remarkable PFOA adsorption capacity of 423 mg/g
384 within 30 minutes and a maximum Langmuir adsorption capacity of 1269 mg/g, due to its increased
385 surface area and hydrophobic nature ⁵⁴.

386 While both acid and alkaline treatments show promise in improving biochar adsorption efficiency,
387 they also come with certain drawbacks. Acid treatments, for instance, can cause severe corrosion
388 of equipment, raising concerns about operational costs and safety. Furthermore, while alkaline
389 treatments increase hydrophobicity, they may also introduce structural weaknesses that could
390 reduce the biochar's durability in long-term applications. There is also limited data on how these
391 treatments affect biochar reusability and potential for secondary pollution, which could limit their
392 sustainability. Hence, further research is needed to optimize these treatments to balance
393 performance, cost, and environmental safety.

394 **Additional functionalization techniques**

395 In addition to what has been stated thus far, biochar can be functionalized using several other
396 methods such as employing peroxides and organic solvents. For instance, functionalizing with

397 hydrogen peroxide can enhance the amount of carboxyl groups found on the biochar surface, thus
398 offering more sites for metal ion adsorption. Methanol can also be used to functionalize biochar by
399 increasing the number of O-containing groups, thereby enhancing tetracycline removal.
400 Furthermore, N-functional groups can be added to the surface of biochar by using N-containing
401 chemicals like urea and melamine. Several treatments, including 3-aminopropyltrimethoxysilane,
402 aniline, and melamine, were employed effectively to boost the N concentration of coffee-ground
403 biochar. Similarly, the addition of methyl diethanolamine increased the N concentration of biochar
404 generated from corncobs. Prior to functionalizing a material for a certain purpose, it is essential to
405 assess the proposed functionalization procedure thoroughly ⁵⁵.

406 However, these methods come with some challenges. For example, while methanol effectively
407 increases oxygen-containing groups, it also increases the risk of organic solvent leaching into
408 treated water, which poses additional environmental challenges. Additionally, the use of N-
409 containing chemicals raises concerns about nutrient leaching and the long-term environmental
410 effects of nitrogen enrichment in water systems. This underscores the need for a more sustainable
411 and eco-friendly approach to biochar functionalization, which has been largely overlooked in the
412 current literature.

413

414 **Variables affecting PFAS removal**

415 **Effect of pH**

416 The pH of the solution plays a pivotal role in the adsorption of PFAS onto biochar, as it directly
417 influences electrostatic forces, hydrophobic effects, and ion exchange mechanisms. **Figure 5**
418 depicts the pH ranges used in various studies on PFAS adsorption using biochar, highlighting the
419 variability in adsorption performance based on the selected pH conditions.

420 At lower pH levels, biochar surfaces tend to have more protonated functional groups, resulting in
421 a positively charged surface. This enhances electrostatic attraction between the negatively charged
422 PFAS molecules, such as PFOS and PFOA, and the biochar, leading to greater adsorption
423 efficiency. For instance, in a study using corn straw biochar with a point of zero charge (pH_{PZC}) of
424 10.3, the sorption capacity of PFOS decreased from 63 to 55 mg/g as the pH increased from 3 to
425 10. This indicates that at lower pH, the positively charged biochar surface creates stronger
426 electrostatic interactions with the negatively charged PFAS molecules, enhancing adsorption ⁵⁶.

427 A similar trend was observed with biochar derived from sawdust and red mud, where PFOS
428 adsorption values were 178.1 mg/g and 194.6 mg/g at a pH of 3.1, respectively, but dropped to 124
429 mg/g and 132 mg/g at a pH of 10.2. This reduction in adsorption capacity is attributed to the
430 diminished positive charge on the biochar surface at higher pH levels, which weakens the
431 electrostatic interactions. However, this suggests a potential limitation when applying biochar in
432 natural environments where pH varies, such as in industrial wastewater. Nevertheless, hydrophobic
433 interactions between the PFOS molecules' fluorinated carbon chains and the biochar surface
434 remained significant, especially at higher pH values, where electrostatic repulsion is more
435 pronounced ⁵⁷.

436 Conversely, at higher pH levels, biochar surfaces become negatively charged due to the
437 deprotonation of functional groups, leading to electrostatic repulsion between the negatively
438 charged PFAS molecules and the biochar surface. This generally reduces adsorption efficiency.
439 However, hydrophobic interactions between the PFAS molecules and the biochar surface continue
440 to play a substantial role, especially for long-chain PFAS. These interactions remain effective even
441 at basic pH levels, compensating to some extent for the reduced electrostatic attraction. This was
442 seen in the study involving sawdust and red mud-derived biochar, where adsorption capacities
443 diminished with rising pH but persisted due to hydrophobic effects^{57,58}.

444 Thus, optimizing the pH during PFAS treatment using biochar is critical. Acidic conditions tend to
445 favor electrostatic interactions, while neutral to basic conditions rely more on hydrophobic
446 interactions. However, the practical challenges of maintaining optimal pH in diverse environmental
447 settings cannot be ignored. A careful balance between these factors can maximize the efficacy of
448 biochar in removing both short- and long-chain PFAS.

449

450 **Effect of chain length**

451 According to previous research, the adsorption distribution coefficient (K_d) of PFAS increases with
452 the length of the perfluorinated carbon chain. This is due to stronger hydrophobic interactions
453 associated with longer chains. The perfluorinated tail, with a larger surface area, requires more free
454 energy for cavity formation in water, leading to stronger adsorption behavior. Long-chain PFAS
455 compounds demonstrate a higher affinity for biochar adsorption compared to shorter-chain
456 compounds. For example, biochar derived from biosolids was able to capture over 80% of long-
457 chain PFAS but only 19-27% of short-chain PFAS. This is attributed to the higher hydrophobicity
458 and stronger interactions of long-chain PFAS with biochar surfaces⁵⁹.

459 Du et al. (2014) highlighted those hydrophobic interactions, including van der Waals forces, play
460 a key role in the sorption of long-chain PFAS ($>C_6$) onto biochar⁶⁰. In contrast, shorter-chain PFAS
461 are influenced more by electrostatic interactions, which tend to result in weaker sorption.
462 Supporting this, Higgins and Luthy (2006) found that long-chain PFAS exhibit stronger sorption
463 to sediments compared to shorter chains. Vo et al. (2022) noted that $\log K_d$ values for long-chain
464 PFAS ranged between 0.77 and 4.63, whereas for short-chain PFAS, the $\log K_d$ remained below
465 0.68⁶¹.

466 The hydrophobicity of PFAS is an important factor in their adsorption, and this property increases
467 with the length of the carbon chain. This is quantified by the octanol-water partition coefficient
468 ($\log K_{ow}$), which measures the compound's tendency to partition between water and organic
469 phases. Fabregat-Palau et al. (2022) reported a linear increase in hydrophobicity with each
470 additional CF_2 unit, corresponding to an increase of 0.5 $\log K_{ow}$ per CF_2 for perfluoro carboxylic
471 acids (PFCAs) and 0.8 $\log K_{ow}$ per CF_2 for perfluoro sulfonic acids (PFSAs)^{62, 63}.

472 **Effect of pyrolysis temperature**

473 **Figure 6** depicts the pyrolysis temperature selected for biochar in the PFAS adsorption literature
474 published to date. Corn straw TG-DTG curves were utilized by Guo et al. (2017) to examine the

475 non-condensable gases and biochar residue during biochar production [51]. The biochar
476 preparation temperatures used in their study (250, 400, 550, and 700°C) aligned with different
477 stages of hemicellulose and cellulose decomposition. At lower temperatures (250°C),
478 hemicellulose partially decomposed, while at 400°C, hemicellulose was fully decomposed, and
479 cellulose began decomposing. Temperatures at 550°C and 700°C resulted in complete
480 decomposition of both hemicellulose and cellulose, producing highly carbonized biochar. Biochar
481 produced at 700°C (BC700) displayed a cleaner surface compared to that produced at lower
482 temperatures, as confirmed by studies using straw and pine wood biochar. At lower pyrolysis
483 temperatures, incomplete decomposition results in residual organic matter coating the biochar
484 surface. These residues can obstruct pore structures and create a less-defined surface morphology.
485 Conversely, at higher temperatures, such as 700°C, the thermal energy is sufficient to drive off
486 these residues, leaving a cleaner, more developed pore structure ⁶⁴.

487 Guo et al. also found that increasing the pyrolysis temperature from 250°C to 700°C decreased the
488 biochar yield but increased the ash content. The proportion of organic carbon increased, and the
489 H/C ratio decreased, leading to higher aromaticity and lower polarity. The specific surface area
490 (SSA) of the biochar also increased with temperature, indicating a higher degree of pore formation.
491 This is critical because PFAS adsorption is strongly influenced by both the availability of
492 micropores and surface hydrophobicity. The adsorption of PFOS was reported to be hydrophobic
493 in nature, and this was enhanced at higher pyrolytic temperatures [53]. Among the biochars, BC700
494 exhibited the highest PFOS adsorption capacity (169.30 mg/g), attributed to its higher abundance
495 of aromatic and non-polar groups. Furthermore, elevated temperatures led to an increase in
496 aromatic ring C=O and C-H groups, which reduced the number of polar groups on the biochar
497 surface, further enhancing its hydrophobicity and making it more favorable for PFOS adsorption
498 ⁶⁵.

499
500 Wang et al. (2023) expanded on these findings by examining biochar produced at pyrolysis
501 temperatures of 300°C, 400°C, 500°C, and 600°C for PFAS remediation. They observed that as the
502 pyrolysis temperature increased, the O/C ratio of the biochar decreased from 0.250 to 0.0553, while
503 the H/C ratio dropped from 0.785 to 0.251. This indicates that the biochar became more aromatic
504 and less polar as temperature increased. The specific surface area (SSA), measured using CO₂
505 adsorption, increased significantly from 219 to 698 m²/g as the pyrolysis temperature rose. This
506 increase in surface area, coupled with a more condensed aromatic structure, boosted the biochar
507 adsorption capacity, as reflected in the higher K_D values observed for biochar pyrolyzed at 600°C
508 ⁶⁶.

509 Overall, these findings show that higher pyrolysis temperatures lead to more carbonized biochar
510 with increased surface area, porosity, and hydrophobicity, which generally enhance PFAS removal
511 performance. However, excessively high pyrolysis conditions may lead to diminishing returns in
512 certain environmental contexts. For instance, very high pyrolysis temperatures (above ~700°C) can
513 sometimes reduce micropore volume through sintering, which could negatively affect the
514 adsorption of short-chain PFAS. Short-chain PFAS typically rely more on electrostatic and weaker
515 hydrophobic interactions, which may be less effective with highly carbonized biochar. Therefore,
516 optimizing pyrolysis temperature based on the specific application, biochar feedstock, and PFAS

517 chain length is crucial. Moreover, the high energy costs associated with extreme pyrolysis
518 temperatures may limit the scalability of this approach for large-scale environmental applications,
519 creating a trade-off between biochar effectiveness and economic feasibility, which has not been
520 adequately addressed in much of the current literature.

521 **Effect of particle size**

522 Particle size of biochar is a critical parameter influencing PFAS sorption capacity in biochar.
523 **Figure 7** presents the biochar particle sizes reported in the literature for PFAS adsorption. Smaller
524 particles generally exhibit higher adsorption capacities due to increased surface area and exposure
525 of more active sites. Hassan et al. (2020) demonstrated that biochar with smaller particle sizes (0.5
526 mm) showed significantly enhanced PFOS adsorption compared to larger particles (up to 2 mm).
527 This increase in adsorption is attributed to the greater surface area and more accessible sorption
528 sites ⁶⁷.

529 Similarly, Xiao et al. (2017) found that PFOS and PFOA removal improved with finer particles,
530 indicating that smaller particles reduce intraparticle diffusion limitations, thus enhancing sorption
531 efficiency. However, larger particles may suffer from slower adsorption kinetics due to diffusion
532 constraints. Despite these advantages, smaller particles may pose operational challenges in large-
533 scale systems, including difficulties in separation, regeneration, and the risk of clogging in filtration
534 setups. Therefore, an optimal particle size needs to be selected to balance sorption performance and
535 practical feasibility in real-world applications ⁶⁸.

536

537 **Effect of competitive sorption**

538 In order to examine how co-existing compounds affect PFASs sorption, Zhang et al (2019) studied
539 the removal of PFOA, PFBS, PFOS, and PFBA in both single and mixed solutions using biochar
540 ⁶⁹. Biochar was more effective at removing PFASs in Single-solution rather than mixed-solution,
541 according to the results. PFAS removal efficiencies decreased by 32.8% to 57.9% in mixed-
542 solutions, indicating competitive PFAS sorption throughout the sorption procedure. As previously
543 reported ³⁷, this competition between co-existing compounds and PFASs on the adsorbent surface
544 could contribute to slow kinetics for PFASs adsorption, like pore block and diffusion-controlled
545 transport into the pores of the adsorbent. As mentioned previously, in the presence of co-existing
546 compounds, long-chain PFASs were preferentially adsorbed onto the sorbents due to their greater
547 hydrophobic interaction than short chains ⁶⁹.

548 While previous studies provided valuable insights, it is important to note that real-world scenarios,
549 particularly in wastewater treatment, often involve complex mixtures of contaminants. For
550 instance, real wastewater matrices contain natural organic matter (NOM), which could further
551 interfere with PFAS sorption efficiency. This highlights a gap in the study where the potential
552 impacts of NOM or other ubiquitous contaminants were not considered.

553 **Effect of biochar dosage**

554 The dosage of biochar is a key factor influencing PFAS adsorption, as numerous studies
555 demonstrate a strong correlation between sorbent dosage and removal efficiency. However, there

556 is an optimal dosage beyond which additional biochar does not significantly improve removal.
557 Once this point is exceeded, the availability of active sites diminishes due to particle aggregation
558 or diffusion limitations, reducing the overall sorption capacity ⁷⁰¹⁹.

559 At lower concentrations, smaller dosages can achieve effective removal, while higher
560 concentrations require more biochar to ensure sufficient active site coverage. Additionally, higher
561 dosages may initially accelerate adsorption, as observed in studies where increasing the biochar
562 dosage significantly improved adsorption rates. However, excessive amounts can lead to
563 diminishing returns, with reduced overall efficiency due to the saturation of available sites and
564 physical limitations ⁷¹⁷².

565 **Challenges in Scaling Functionalized Biochar for PFAS Remediation**

566 The large-scale implementation of functionalized biochar for the remediation PFAS presents
567 multifaceted challenges spanning technical, environmental, economic, and regulatory domains.

568 **Technical Challenges**

569 The efficacy of biochar in adsorbing PFAS is influenced by the chain length of the compounds.
570 Studies demonstrate that biochar exhibits reduced removal efficiency for short-chain PFAS
571 compared to long-chain counterparts, necessitating the development of tailored functionalization
572 strategies to enhance adsorption across diverse PFAS structures ⁷³.

573 The physicochemical properties of biochar, including pore structure and functional groups, are
574 highly dependent on the feedstock and pyrolysis conditions. This variability can lead to inconsistent
575 performance, underscoring the need for standardized production protocols to ensure uniform
576 efficacy in PFAS remediation.

577 Developing efficient and cost-effective regeneration techniques for spent biochar remains an active
578 area of research. Current methods, such as thermal treatment and solvent extraction, are often
579 energy-intensive or environmentally taxing, making them impractical for large-scale real-world
580 applications ⁷⁴.

581 **Environmental Challenges**

582 The environmental sustainability of biochar production is influenced by the carbon footprint
583 associated with pyrolysis processes, which vary based on biomass type and energy inputs.
584 Mitigation strategies, including the use of renewable energy sources and optimization of pyrolysis
585 parameters, are essential to minimize greenhouse gas emissions and enhance the overall
586 environmental benefits of biochar application ⁷⁵.

587 The improper disposal of PFAS-laden biochar poses a risk of secondary contamination to soil and
588 water systems. Ensuring the safe handling, stabilization, and disposal of spent biochar is critical to
589 prevent the re-release of adsorbed PFAS into the environment.

590

591 **Economic Challenges**

592 Although biochar is generally affordable, the functionalization processes required for PFAS
593 remediation significantly increase costs. Scaling up these processes also incurs additional expenses
594 for transportation, storage, and specialized application equipment.

595 The transition from laboratory-scale studies to full-scale applications introduces challenges in
596 maintaining cost-effectiveness and operational efficiency. Addressing scalability concerns requires
597 comprehensive pilot studies and the development of standardized protocols to ensure consistent
598 performance across varying operational contexts ⁷⁶.

599 **Regulatory Challenges**

600 The use of certain functionalization agents, such as nanoparticles, may pose environmental or
601 health risks. Comprehensive risk assessments and the development of safer functionalization
602 methods are necessary to meet regulatory standards ¹².

603 Addressing these challenges requires a multidisciplinary approach, integrating advancements in
604 material science, environmental engineering, economics, and policy development to realize the
605 potential of functionalized biochar for PFAS remediation at scale.

606 **Conclusions, gaps, and future perspectives**

607 Numerous studies on environmental remediation are now concentrating on biochars and functiona
608 lized biochars. Their extensive availability, cost-effectiveness, environmental acceptability, and
609 significant sorption capacity make them appropriate for the sorption of numerous pollutant species.
610 Based on the pollutant type and the technique used for generating the biochar, however, their
611 adsorption capability varies significantly. Therefore, selecting the proper biochar for the
612 appropriate pollutants is essential. In addition, a single type of biochar is probably insufficient to
613 remove all categories of pollutants. Porosity, surface charge, pH, surface area, functional groups,
614 and mineral content are physicochemical properties that affect the adsorption capacity of biochar.
615 Therefore, the features of biochar must be comprehended and accounted for.

616 This paper reports a comprehensive analysis of the utilization of biochar to eliminate contaminants.
617 The manuscript encompasses diverse parts, including the classification of biochar, the utilization
618 of pristine and functionalized biochar for the removal of pollutants, and the eradication of PFASs
619 and related techniques. In addition to highlighting the limitations and high costs of traditional
620 contaminant removal methods, this article presents biochar as a promising alternative. This paper
621 summarizes previous research on the application of pristine and functionalized biochar for PFAS
622 removal and identifies key variables that influence the efficacy of this technique. Given that the
623 utilization of biochar for PFAS removals a relatively new discipline, the paper suggests that
624 additional research is necessary for the cases listed below.

- 625 – There are several types of functionalization strategies for improving the sorption capacity of
626 biochar. Nevertheless, few studies have been conducted in this field, and the majority of
627 research has employed unmodified biochar for removing PFAS contaminants. Therefore,
628 additional research on the functionalization of biochar is required prior to its implementation
629 for removal goals.

630

- 631 – Few investigations have been devoted to short-chain PFAS, and the available research shows
632 that their removal efficacy is declining. Future research should prioritize the increased removal
633 of short-chain PFAS compounds and expand its reach to include a wider variety of PFAS
634 species in order to address this problem. This is especially crucial given that short-chain PFASs
635 are anticipated to become more common in the environment as long-chain PFAS are replaced
636 by them.
- 637
- 638 – To enhance the removal efficiency of short-chain PFAS, future research should explore the
639 synergistic use of biochar with other treatment methods. For instance, coupling biochar
640 adsorption with degradation techniques, such as advanced oxidation processes, photocatalysis,
641 or enzymatic treatments, can improve the overall efficiency of PFAS remediation. Developing
642 a framework that combines multiple treatment strategies will allow for the simultaneous
643 capture and breakdown of PFAS, addressing both the persistence and mobility of these
644 contaminants. This approach could offer a more comprehensive solution, particularly in real-
645 world applications where PFAS co-exist with other pollutants in complex matrices.
- 646 – Machine learning, artificial intelligence, and data analytics are relatively new fields. The vast
647 amount of data generated by biochar studies related to remediation necessitates the
648 development of decision-making tools based on data-driven modelling, deep learning, and
649 artificial intelligence. This will aid in the design, scalability, and development of biochar
650 utilization for PFASs remediation. To accomplish this, a framework for incorporating AI and
651 machine learning into the use of biochar has been proposed.
- 652 – To ascertain the sorption capacity of biochar, additional research is required. While some
653 research has been conducted in this area, comparison is difficult because adsorption capacities
654 have been measured in a variety of methods, including batch experiments and column modes.
655 In addition, the preparation conditions for biochar adsorbents, such as temperature, time, and
656 atmosphere, vary greatly, which further complicates efforts to compare them.
- 657 – Utilizing economical and eco-friendly modifiers, like industrial solid residues, could provide a
658 viable future development path for reducing costs and promoting environmental sustainability.
659 These pollutants include phosphogypsum, tailings, red mud, coal gangue, fly ash, and etc. By
660 combining the pyrolysis of these industrial solid wastes with biochar raw materials, it is
661 possible to reduce their toxicity while achieving stabilization and resource utilization, thereby
662 reducing their negative environmental impact.
- 663 – Most studies on functionalized biochars have been conducted under controlled laboratory
664 conditions, limiting their applicability to real wastewater systems. Future research should
665 emphasize pilot-scale studies and field trials to evaluate the performance of biochar in the
666 presence of co-contaminants and varying water chemistries. Addressing these operational
667 challenges will help bridge the gap between laboratory findings and practical implementation
668 in large-scale wastewater treatment systems.

669

670 Acknowledgement:

671 This research was funded by the Natural Sciences and Engineering Research Council (Discovery
672 Grant 23451, NSERC Alliance Option-2 Grants MISSED Project, ALLRP 571066–21). We would

673 also like to thank James and Joanne Love Chair in Environmental Engineering, for their financial
674 support.

675

676 **Declaration of interests**

677 The authors declare no competing interests.

678

679

680 **Figure Titles**

681 **Figure 1.** Frequency of biochar characterization techniques in PFAS removal studies

682 **Figure 2.** a) The number of publications in the field of PFAS removal using biochar, b) The
683 quantity of various PFAS contaminants eliminated by biochar

684 **Figure 3.** Word cloud of the keywords used in articles about PFAS removal utilizing biochar.

685 **Figure 4.** The techniques employed so far to functionalize biochar for removing PFASs.

686 **Figure 5.** The pH range of studies investigating biochar's capacity for PFAS removal.

687

688 **Figure 6.** The pyrolysis temperature selected for biochar in the currently available literature for
689 PFAS sorption.

690 **Figure 7.** Biochar particle sizes reported in the literature for PFAS adsorption.

691

692

693

694 **References**

- 695 1. Yuan, P., Wang, J., Pan, Y., Shen, B., and Wu, C. (2018). Review of biochar for the management of
696 contaminated soil: Preparation, application and prospect. *Science of The Total Environment* 659,
697 473–490.
- 698 2. Qiu, M., Liu, L., Ling, Q., Cai, Y., Yu, S., Wang, S., Fu, D., Hu, B., and Wang, X. (2022). Biochar for
699 the removal of contaminants from soil and water: a review. *Biochar* 4, 1–25.
700 <https://doi.org/10.1007/S42773-022-00146-1/FIGURES/7>.
- 701 3. Banks, D., Jun, B.M., Heo, J., Her, N., Park, C.M., and Yoon, Y. (2020). Selected advanced water
702 treatment technologies for perfluoroalkyl and polyfluoroalkyl substances: A review. *Sep Purif*
703 *Technol* 231. <https://doi.org/10.1016/J.SEPPUR.2019.115929>.

- 704 4. Behnami, A., Pourakbar, M., Ayyar, A.S.R., Lee, J.W., Gagnon, G., and Zoroufchi Benis, K. (2024).
705 Treatment of aqueous per- and poly-fluoroalkyl substances: A review of biochar adsorbent
706 preparation methods. *Chemosphere* 357, 142088.
707 <https://doi.org/10.1016/J.CHEMOSPHERE.2024.142088>.
- 708 5. Cordner, A., De La Rosa, V.Y., Schaidler, L.A., Rudel, R.A., Richter, L., and Brown, P. (2019).
709 Guideline levels for PFOA and PFOS in drinking water: the role of scientific uncertainty, risk
710 assessment decisions, and social factors. *J Expo Sci Environ Epidemiol* 29, 157–171.
711 <https://doi.org/10.1038/S41370-018-0099-9>.
- 712 6. Dabbaghi, F., Nasrollahpour, S., Dehestani, M., and Yousefpour, H. (2021). Optimization of
713 Concrete Mixtures Containing Lightweight Expanded Clay Aggregates Based on Mechanical,
714 Economical, Fire-Resistance, and Environmental Considerations. *Journal of Materials in Civil
715 Engineering* 34, 04021445. [https://doi.org/10.1061/\(ASCE\)MT.1943-5533.0004083](https://doi.org/10.1061/(ASCE)MT.1943-5533.0004083).
- 716 7. Nasrollahpour, S., Kebria, D.Y., Ghavami, M., and Ghasemi-Fare, O. (2020). Application of
717 Organically Modified Clay in Removing BTEX from Produced Water. 275–283.
718 <https://doi.org/10.1061/9780784482827.031>.
- 719 8. Zhang, J., Pang, H., Gray, S., Ma, S., Xie, Z., and Gao, L. (2021). Pfas removal from wastewater by
720 in-situ formed ferric nanoparticles: Solid phase loading and removal efficiency. *J Environ Chem
721 Eng* 9. <https://doi.org/10.1016/J.JECE.2021.105452>.
- 722 9. Ahmed, M.B., Alam, M.M., Zhou, J.L., Xu, B., Johir, M.A.H., Karmakar, A.K., Rahman, M.S., Hossen,
723 J., Hasan, A.T.M.K., and Moni, M.A. (2020). Advanced treatment technologies efficacies and
724 mechanism of per- and poly-fluoroalkyl substances removal from water. *Process Safety and
725 Environmental Protection* 136, 1–14. <https://doi.org/10.1016/j.psep.2020.01.005>.
- 726 10. Nasrollahpour, S., Tanhadoust, A., Pulicharla, R., and Brar, S.K. (2024). Long-chain perfluoroalkyl
727 carboxylic acids removal by biochar: Experimental study and uncertainty based data-driven
728 predictive model. *iScience* 27, 111140. <https://doi.org/10.1016/j.isci.2024.111140>.
- 729 11. Nasrollahpour, S., Kebria, D.Y., Nehdi, M.L., Tanhadoust, A., and Ghavami, M. (2023).
730 Remediation of NAPL-Contaminated Brackish Water by Synthesized Organoclay: Experimental
731 Analysis and BNN Predictive Model. *J Hazard Toxic Radioact Waste* 27, 04023028.
732 <https://doi.org/10.1061/JHTRBP.HZENG-1212>.
- 733 12. Qiu, M., Liu, L., Ling, Q., Cai, Y., Yu, S., Wang, S., Fu, D., Hu, B., and Wang, X. (2022). Biochar for
734 the removal of contaminants from soil and water: a review. *Biochar* 4, 1–25.
735 <https://doi.org/10.1007/S42773-022-00146-1/FIGURES/7>.
- 736 13. Jin, X., Liu, R., Wang, H., Han, L., Qiu, M., and Hu, B. (2022). Functionalized porous nanoscale
737 Fe₃O₄ particles supported biochar from peanut shell for Pb(II) ions removal from landscape
738 wastewater. *Environmental Science and Pollution Research* 29, 37159–37169.
739 <https://doi.org/10.1007/S11356-021-18432-Z/FIGURES/9>.
- 740 14. Qiu, M., Hu, B., Chen, Z., Yang, H., Zhuang, L., and Wang, X. (2021). Challenges of organic
741 pollutant photocatalysis by biochar-based catalysts. *Biochar* 3, 117–123.
742 <https://doi.org/10.1007/S42773-021-00098-Y>.

- 743 15. Ross, I., Mcdonough, J., Miles, J., Storch, P., Kochunarayanan, P.T., Kalve, E., Hurst, J., Dasgupta,
744 S.S., and Burdick, J. (2018). A review of emerging technologies for remediation of PFASs.
745 <https://doi.org/10.1002/rem.21553>.
- 746 16. Navarathna, C., Keel, M.G., Rodrigo, P.M., Carrasco, C., Ramirez, A., Jamison, H., Mlsna, T.E., and
747 Mohan, D. (2022). Biochar and biochar composites for poly- and perfluoroalkyl substances (PFAS)
748 sorption. *Sustainable Biochar for Water and Wastewater Treatment*, 555–595.
749 <https://doi.org/10.1016/B978-0-12-822225-6.00005-1>.
- 750 17. Tanhadoust, A., Yang, T.Y., Dabbaghi, F., Chai, H.K., Mohseni, M., Emadi, S.B., and Nasrollahpour,
751 S. (2023). Predicting stress-strain behavior of normal weight and lightweight aggregate concrete
752 exposed to high temperature using LSTM recurrent neural network. *Constr Build Mater* 362.
753 <https://doi.org/10.1016/J.CONBUILDMAT.2022.129703>.
- 754 18. Tanhadoust, A., Emadi, S.A.A., Nasrollahpour, S., Dabbaghi, F., and Nehdi, M.L. (2023). Optimal
755 design of sustainable recycled rubber-filled concrete using life cycle assessment and multi-
756 objective optimization. *Constr Build Mater* 402, 132878.
757 <https://doi.org/10.1016/J.CONBUILDMAT.2023.132878>.
- 758 19. Zeghioud, H., Fryda, L., Djelal, H., Assadi, A., and Kane, A. (2022). A comprehensive review of
759 biochar in removal of organic pollutants from wastewater: Characterization, toxicity,
760 activation/functionalization and influencing treatment factors. *Journal of Water Process*
761 *Engineering* 47. <https://doi.org/10.1016/J.JWPE.2022.102801>.
- 762 20. Dabbaghi, F., Fallahnejad, H., Nasrollahpour, S., Dehestani, M., and Yousefpour, H. (2021).
763 Evaluation of fracture energy, toughness, brittleness, and fracture process zone properties for
764 lightweight concrete exposed to high temperatures. *Theoretical and Applied Fracture Mechanics*
765 116, 103088. <https://doi.org/10.1016/J.TAFMEC.2021.103088>.
- 766 21. Cai, S., Zhang, Q., Wang, Z., Hua, S., Ding, D., Cai, T., and Zhang, R. (2021). Pyrrolic N-rich biochar
767 without exogenous nitrogen doping as a functional material for bisphenol A removal:
768 Performance and mechanism. *Appl Catal B* 291. <https://doi.org/10.1016/J.APCATB.2021.120093>.
- 769 22. Xiong, S., Deng, Y., Tang, R., Zhang, C., Zheng, J., Zhang, Y., Su, L., Yang, L., Liao, C., and Gong, D.
770 (2020). Factors study for the removal of epoxiconazole in water by common biochars. *Biochem*
771 *Eng J* 161. <https://doi.org/10.1016/J.BEJ.2020.107690>.
- 772 23. Ma, X., Zhou, B., Budai, A., Jeng, A., Hao, X., Wei, D., Zhang, Y., and Rasse, D. (2016). Study of
773 Biochar Properties by Scanning Electron Microscope – Energy Dispersive X-Ray Spectroscopy
774 (SEM-EDX). *Commun Soil Sci Plant Anal* 47, 593–601.
775 <https://doi.org/10.1080/00103624.2016.1146742>.
- 776 24. Zhang, P., O’Connor, D., Wang, Y., Jiang, L., Xia, T., Wang, L., Tsang, D.C.W., Ok, Y.S., and Hou, D.
777 (2020). A green biochar/iron oxide composite for methylene blue removal. *J Hazard Mater* 384.
778 <https://doi.org/10.1016/J.JHAZMAT.2019.121286>.
- 779 25. Al-Wabel, M.I., Ahmad, M., Usman, A.R.A., and Al-Farraj, A.S.F. (2021). Designing chitosan based
780 magnetic beads with conocarpus waste-derived biochar for efficient sulfathiazole removal from
781 contaminated water. *Saudi J Biol Sci* 28, 6218–6229. <https://doi.org/10.1016/J.SJBS.2021.06.072>.

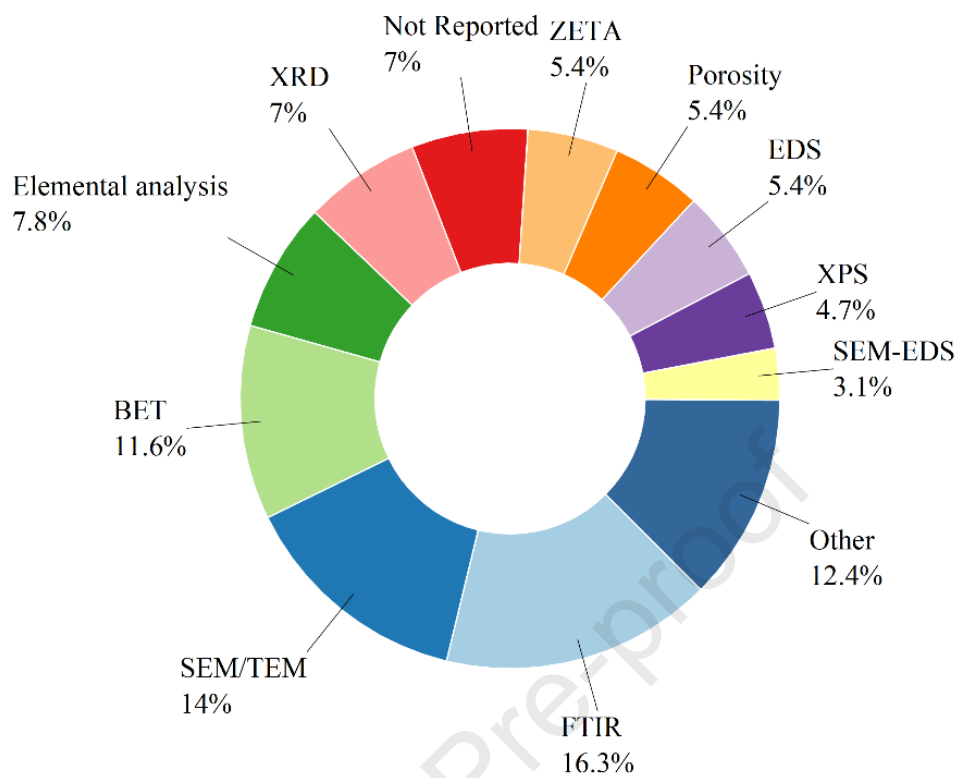
- 782 26. Hu, B., Tang, Y., Wang, X., Wu, L., Nong, J., Yang, X., and Guo, J. (2021). Cobalt-gadolinium
783 modified biochar as an adsorbent for antibiotics in single and binary systems. *Microchemical*
784 *Journal* 166. <https://doi.org/10.1016/J.MICROC.2021.106235>.
- 785 27. Kim, J.E., Bhatia, S.K., Song, H.J., Yoo, E., Jeon, H.J., Yoon, J.Y., Yang, Y., Gurav, R., Yang, Y.H., Kim,
786 H.J., et al. (2020). Adsorptive removal of tetracycline from aqueous solution by maple leaf-
787 derived biochar. *Bioresour Technol* 306. <https://doi.org/10.1016/J.BIORTECH.2020.123092>.
- 788 28. Hassan, M.M., and Carr, C.M. (2018). A critical review on recent advancements of the removal of
789 reactive dyes from dyehouse effluent by ion-exchange adsorbents. *Chemosphere* 209, 201–219.
790 <https://doi.org/10.1016/J.CHEMOSPHERE.2018.06.043>.
- 791 29. Yang, X., Zhang, S., Ju, M., and Liu, L. (2019). Preparation and modification of biochar materials
792 and their application in soil remediation. *Applied Sciences (Switzerland)* 9.
793 <https://doi.org/10.3390/APP9071365>.
- 794 30. Qiu, M., Liu, L., Ling, Q., Cai, Y., Yu, S., Wang, S., Fu, D., Hu, B., and Wang, X. (2022). Biochar for
795 the removal of contaminants from soil and water: a review. *Biochar* 4, 1–25.
796 <https://doi.org/10.1007/S42773-022-00146-1/FIGURES/7>.
- 797 31. Amalina, F., Razak, A.S.A., Krishnan, S., Zularisam, A.W., and Nasrullah, M. (2022). A
798 comprehensive assessment of the method for producing biochar, its characterization, stability,
799 and potential applications in regenerative economic sustainability – A review. *Cleaner Materials*
800 3. <https://doi.org/10.1016/J.CLEMA.2022.100045>.
- 801 32. Chen, H., Sun, R., Zhang, C., Han, J., Wang, X., Han, G., and He, X. (2016). Occurrence, spatial and
802 temporal distributions of perfluoroalkyl substances in wastewater, seawater and sediment from
803 Bohai Sea, China. *Environ Pollut* 219, 389–398. <https://doi.org/10.1016/J.ENVPOL.2016.05.017>.
- 804 33. Militao, I.M., Roddick, F.A., Bergamasco, R., and Fan, L. (2021). Removing PFAS from aquatic
805 systems using natural and renewable material-based adsorbents: A review. *J Environ Chem Eng* 9.
806 <https://doi.org/10.1016/J.JECE.2021.105271>.
- 807 34. Franke, V., McCleaf, P., Lindegren, K., and Ahrens, L. (2019). Efficient removal of per- And
808 polyfluoroalkyl substances (PFASs) in drinking water treatment: Nanofiltration combined with
809 active carbon or anion exchange. *Environ Sci (Camb)* 5, 1836–1843.
810 <https://doi.org/10.1039/C9EW00286C>.
- 811 35. Yao, Y., Volchek, K., Brown, C.E., Robinson, A., and Obal, T. (2014). Comparative study on
812 adsorption of perfluorooctane sulfonate (PFOS) and perfluorooctanoate (PFOA) by different
813 adsorbents in water. *Water Science and Technology* 70, 1983–1991.
814 <https://doi.org/10.2166/WST.2014.445>.
- 815 36. Guo, W., Huo, S., Feng, J., and Lu, X. (2017). Adsorption of perfluorooctane sulfonate (PFOS) on
816 corn straw-derived biochar prepared at different pyrolytic temperatures. *J Taiwan Inst Chem Eng*
817 78, 265–271. <https://doi.org/10.1016/J.JTICE.2017.06.013>.

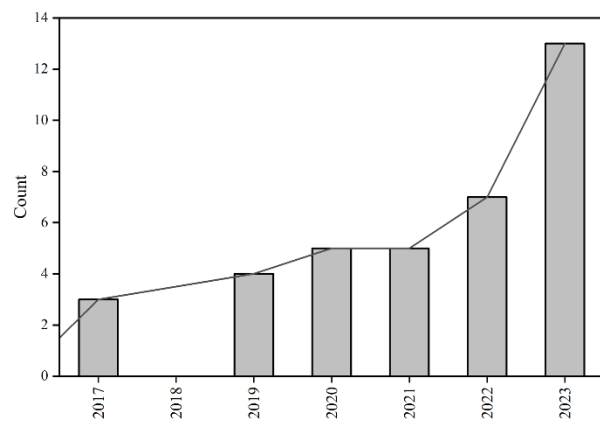
- 818 37. Inyang, M., and Dickenson, E.R.V. (2017). The use of carbon adsorbents for the removal of
819 perfluoroalkyl acids from potable reuse systems. *Chemosphere* 184, 168–175.
820 <https://doi.org/10.1016/J.CHEMOSPHERE.2017.05.161>.
- 821 38. Zhang, D., He, Q., Wang, M., Zhang, W., and Liang, Y. (2021). Sorption of perfluoroalkylated
822 substances (PFASs) onto granular activated carbon and biochar. *Environmental Technology*
823 (United Kingdom) 42, 1798–1809. <https://doi.org/10.1080/09593330.2019.1680744>.
- 824 39. Chen, X., Xia, X., Wang, X., Qiao, J., and Chen, H. (2011). A comparative study on sorption of
825 perfluorooctane sulfonate (PFOS) by chars, ash and carbon nanotubes. *Chemosphere* 83, 1313–
826 1319. <https://doi.org/10.1016/J.CHEMOSPHERE.2011.04.018>.
- 827 40. Tan, X. fei, Liu, Y. guo, Gu, Y. ling, Xu, Y., Zeng, G. ming, Hu, X. jiang, Liu, S. bo, Wang, X., Liu, S.
828 mian, and Li, J. (2016). Biochar-based nano-composites for the decontamination of wastewater:
829 A review. *Bioresour Technol* 212, 318–333. <https://doi.org/10.1016/J.BIORTECH.2016.04.093>.
- 830 41. Thines, K.R., Abdullah, E.C., Mubarak, N.M., and Ruthiraan, M. (2017). Synthesis of magnetic
831 biochar from agricultural waste biomass to enhancing route for waste water and polymer
832 application: A review. *Renewable and Sustainable Energy Reviews* 67, 257–276.
833 <https://doi.org/10.1016/J.RSER.2016.09.057>.
- 834 42. Hassan, M., Liu, Y., Naidu, R., Du, J., and Qi, F. (2020). Adsorption of Perfluorooctane sulfonate
835 (PFOS) onto metal oxides modified biochar. *Environ Technol Innov* 19.
836 <https://doi.org/10.1016/J.ETI.2020.100816>.
- 837 43. Niu, B., Yang, S., Li, Y., Zang, K., Sun, C., Yu, M., Zhou, L., and Zheng, Y. (2020). Regenerable
838 magnetic carbonized *Calotropis gigantea* fiber for hydrophobic-driven fast removal of
839 perfluoroalkyl pollutants. *Cellulose* 27, 5893–5905. <https://doi.org/10.1007/S10570-020-03192-9>.
- 841 44. Tang, J., Lv, H., Gong, Y., and Huang, Y. (2015). Preparation and characterization of a novel
842 graphene/biochar composite for aqueous phenanthrene and mercury removal. *Bioresour*
843 *Technol* 196, 355–363. <https://doi.org/10.1016/J.BIORTECH.2015.07.047>.
- 844 45. Yang, M., Zhang, X., Yang, Y., Liu, Q., Nghiem, L.D., Guo, W., and Ngo, H.H. (2022). Effective
845 destruction of perfluorooctanoic acid by zero-valent iron laden biochar obtained from
846 carbothermal reduction: Experimental and simulation study. *Science of the Total Environment*
847 805. <https://doi.org/10.1016/J.SCITOTENV.2021.150326>.
- 848 46. Zhou, L., Huang, Y., Qiu, W., Sun, Z., Liu, Z., and Song, Z. (2017). Adsorption properties of nano-
849 MnO₂-biochar composites for copper in aqueous solution. *Molecules* 22.
850 <https://doi.org/10.3390/MOLECULES22010173>.
- 851 47. Zhou, L., Huang, Y., Qiu, W., Sun, Z., Liu, Z., and Song, Z. (2017). Adsorption properties of nano-
852 MnO₂-biochar composites for copper in aqueous solution. *Molecules* 22.
853 <https://doi.org/10.3390/MOLECULES22010173>.

- 854 48. Panwar, N.L., and Pawar, A. (2022). Influence of activation conditions on the physicochemical
855 properties of activated biochar: a review. *Biomass Convers Biorefin* 12, 925–947.
856 <https://doi.org/10.1007/S13399-020-00870-3>.
- 857 49. Islam, M.S., Kwak, J.H., Nzediegwu, C., Wang, S., Palansuriya, K., Kwon, E.E., Naeth, M.A., El-Din,
858 M.G., Ok, Y.S., and Chang, S.X. (2021). Biochar heavy metal removal in aqueous solution depends
859 on feedstock type and pyrolysis purging gas. *Environmental Pollution* 281, 117094.
860 <https://doi.org/10.1016/J.ENVPOL.2021.117094>.
- 861 50. Ammar, N.S., Fathy, N.A., Ibrahim, H.S., and Mousa, S.M. (2021). Micro-mesoporous modified
862 activated carbon from corn husks for removal of hexavalent chromium ions. *Appl Water Sci* 11,
863 1–12. <https://doi.org/10.1007/S13201-021-01487-1/FIGURES/11>.
- 864 51. Islam, M.S., Kwak, J.H., Nzediegwu, C., Wang, S., Palansuriya, K., Kwon, E.E., Naeth, M.A., El-Din,
865 M.G., Ok, Y.S., and Chang, S.X. (2021). Biochar heavy metal removal in aqueous solution depends
866 on feedstock type and pyrolysis purging gas. *Environmental Pollution* 281.
867 <https://doi.org/10.1016/J.ENVPOL.2021.117094>.
- 868 52. Cheng, N., Wang, B., Wu, P., Lee, X., Xing, Y., Chen, M., and Gao, B. (2021). Adsorption of
869 emerging contaminants from water and wastewater by modified biochar: A review.
870 *Environmental pollution* 273. <https://doi.org/10.1016/J.ENVPOL.2021.116448>.
- 871 53. Zeng, H., Zeng, H., Zhang, H., Shahab, A., Zhang, K., Lu, Y., Nabi, I., Naseem, F., and Ullah, H.
872 (2021). Efficient adsorption of Cr (VI) from aqueous environments by phosphoric acid activated
873 eucalyptus biochar. *J Clean Prod* 286. <https://doi.org/10.1016/J.JCLEPRO.2020.124964>.
- 874 54. Zhou, Y., Xu, M., Huang, D., Xu, L., Yu, M., Zhu, Y., and Niu, J. (2021). Modulating hierarchically
875 microporous biochar via molten alkali treatment for efficient adsorption removal of
876 perfluorinated carboxylic acids from wastewater. *Science of the Total Environment* 757.
877 <https://doi.org/10.1016/J.SCITOTENV.2020.143719>.
- 878 55. Medeiros, D.C.C. da S., Nzediegwu, C., Benally, C., Messele, S.A., Kwak, J.H., Naeth, M.A., Ok, Y.S.,
879 Chang, S.X., and Gamal El-Din, M. (2022). Pristine and engineered biochar for the removal of
880 contaminants co-existing in several types of industrial wastewaters: A critical review. *Science of*
881 *the Total Environment* 809. <https://doi.org/10.1016/J.SCITOTENV.2021.151120>.
- 882 56. Guo, W., Lu, S., Shi, J., and Zhao, X. (2019). Effect of corn straw biochar application to sediments
883 on the adsorption of 17 α -ethinyl estradiol and perfluorooctane sulfonate at sediment-water
884 interface. *Ecotoxicol Environ Saf* 174, 363–369. <https://doi.org/10.1016/J.ECOENV.2019.01.128>.
- 885 57. Hassan, M., Liu, Y., Naidu, R., Du, J., and Qi, F. (2020). Adsorption of Perfluorooctane sulfonate
886 (PFOS) onto metal oxides modified biochar. *Environ Technol Innov* 19, 100816.
887 <https://doi.org/10.1016/J.ETI.2020.100816>.
- 888 58. Zhou, Y., Xu, M., Huang, D., Xu, L., Yu, M., Zhu, Y., and Niu, J. (2021). Modulating hierarchically
889 microporous biochar via molten alkali treatment for efficient adsorption removal of
890 perfluorinated carboxylic acids from wastewater. *Science of the Total Environment* 757.
891 <https://doi.org/10.1016/J.SCITOTENV.2020.143719>.

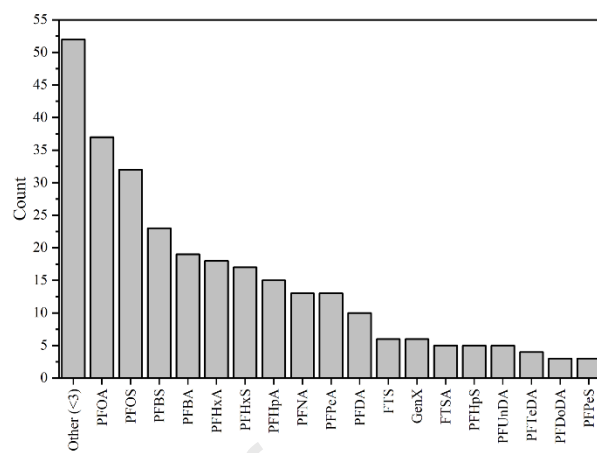
- 892 59. Kundu, S., Patel, S., Halder, P., Patel, T., Hedayati Marzbali, M., Pramanik, B.K., Paz-Ferreiro, J., De
893 Figueiredo, C.C., Bergmann, D., Surapaneni, A., et al. (2021). Removal of PFASs from biosolids
894 using a semi-pilot scale pyrolysis reactor and the application of biosolids derived biochar for the
895 removal of PFASs from contaminated water. *Environ Sci (Camb)* 7, 638–649.
896 <https://doi.org/10.1039/D0EW00763C>.
- 897 60. Du, Z., Deng, S., Bei, Y., Huang, Q., Wang, B., Huang, J., and Yu, G. (2014). Adsorption behavior
898 and mechanism of perfluorinated compounds on various adsorbents-A review. *J Hazard Mater*
899 274, 443–454. <https://doi.org/10.1016/J.JHAZMAT.2014.04.038>.
- 900 61. Vo, H.N.P., Nguyen, T.M.H., Ngo, H.H., Guo, W., and Shukla, P. (2022). Biochar sorption of
901 perfluoroalkyl substances (PFASs) in aqueous film-forming foams-impacted groundwater: Effects
902 of PFASs properties and groundwater chemistry. *Chemosphere* 286, 131622.
903 <https://doi.org/10.1016/J.CHEMOSPHERE.2021.131622>.
- 904 62. Fabregat-Palau, J., Vidal, M., and Rigol, A. Examining sorption of perfluoroalkyl substances (PFAS)
905 in biochars and.
- 906 63. McGregor, R. (2020). Six pilot-scale studies evaluating the in situ treatment of PFAS in
907 groundwater. *Remediation Journal* 30, 39–50. <https://doi.org/10.1002/REM.21653>.
- 908 64. Chen, Z., Chen, B., and Chiou, C.T. (2012). Fast and slow rates of naphthalene sorption to biochars
909 produced at different temperatures. *Environ Sci Technol* 46, 11104–11111.
910 <https://doi.org/10.1021/ES302345E>.
- 911 65. Guo, W., Huo, S., Feng, J., and Lu, X. (2017). Adsorption of perfluorooctane sulfonate (PFOS) on
912 corn straw-derived biochar prepared at different pyrolytic temperatures. *J Taiwan Inst Chem Eng*
913 78, 265–271. <https://doi.org/10.1016/J.JTICE.2017.06.013>.
- 914 66. Wang, Z., Alinezhad, A., Nason, S., Xiao, F., and Pignatello, J.J. (2023). Enhancement of per- and
915 polyfluoroalkyl substances removal from water by pyrogenic carbons: Tailoring carbon surface
916 chemistry and pore properties. *Water Res* 229. <https://doi.org/10.1016/J.WATRES.2022.119467>.
- 917 67. Hassan, M., Liu, Y., Naidu, R., Du, J., and Qi, F. (2020). Adsorption of Perfluorooctane sulfonate
918 (PFOS) onto metal oxides modified biochar. *Environ Technol Innov* 19.
919 <https://doi.org/10.1016/J.ETI.2020.100816>.
- 920 68. Xiao, X., Ulrich, B.A., Chen, B., and Higgins, C.P. (2017). Sorption of Poly- and Perfluoroalkyl
921 Substances (PFASs) Relevant to Aqueous Film-Forming Foam (AFFF)-Impacted Groundwater by
922 Biochars and Activated Carbon. *Environ Sci Technol* 51, 6342–6351.
923 https://doi.org/10.1021/ACS.EST.7B00970/ASSET/IMAGES/LARGE/ES-2017-00970R_0005.JPEG.
- 924 69. Zhang, D., He, Q., Wang, M., Zhang, W., and Liang, Y. (2019). Sorption of perfluoroalkylated
925 substances (PFASs) onto granular activated carbon and biochar. *Environmental Technology*
926 (United Kingdom) 42, 1798–1809. <https://doi.org/10.1080/09593330.2019.1680744>.
- 927 70. Lawal, A.A., Hassan, M.A., Ahmad Farid, M.A., Tengku Yasim-Anuar, T.A., Samsudin, M.H., Mohd
928 Yusoff, M.Z., Zakaria, M.R., Mokhtar, M.N., and Shirai, Y. (2021). Adsorption mechanism and

- 929 effectiveness of phenol and tannic acid removal by biochar produced from oil palm frond using
930 steam pyrolysis. *Environmental Pollution* 269. <https://doi.org/10.1016/J.ENVPOL.2020.116197>.
- 931 71. Vigneshwaran, S., Sirajudheen, P., Nikitha, M., Ramkumar, K., and Meenakshi, S. (2021). Facile
932 synthesis of sulfur-doped chitosan/biochar derived from tapioca peel for the removal of organic
933 dyes: Isotherm, kinetics and mechanisms. *J Mol Liq* 326.
934 <https://doi.org/10.1016/J.MOLLIQ.2021.115303>.
- 935 72. Militao, I.M., Roddick, F., Fan, L., Zepeda, L.C., Parthasarathy, R., and Bergamasco, R. (2023). PFAS
936 removal from water by adsorption with alginate-encapsulated plant albumin and rice straw-
937 derived biochar. *Journal of Water Process Engineering* 53, 103616.
938 <https://doi.org/10.1016/J.JWPE.2023.103616>.
- 939 73. Salawu, O.A., and Adeleye, A.S. (2023). Adsorption of PFAS onto secondary microplastics: A
940 mechanistic study. <https://doi.org/10.26434/CHEMRXIV-2023-NCMVJ>.
- 941 74. Ross, I., Mcdonough, J., Miles, J., Storch, P., Kochunarayanan, P.T., Kalve, E., Hurst, J., Dasgupta,
942 S.S., and Burdick, J. (2018). A review of emerging technologies for remediation of PFASs.
943 <https://doi.org/10.1002/rem.21553>.
- 944 75. Cheng, N., Wang, B., Wu, P., Lee, X., Xing, Y., Chen, M., and Gao, B. (2021). Adsorption of
945 emerging contaminants from water and wastewater by modified biochar: A review.
946 *Environmental pollution* 273. <https://doi.org/10.1016/J.ENVPOL.2021.116448>.
- 947 76. Navarathna, C., Keel, M.G., Rodrigo, P.M., Carrasco, C., Ramirez, A., Jamison, H., Mlsna, T.E., and
948 Mohan, D. (2022). Biochar and biochar composites for poly- and perfluoroalkyl substances (PFAS)
949 sorption. *Sustainable Biochar for Water and Wastewater Treatment*, 555–595.
950 <https://doi.org/10.1016/B978-0-12-822225-6.00005-1>.
- 951

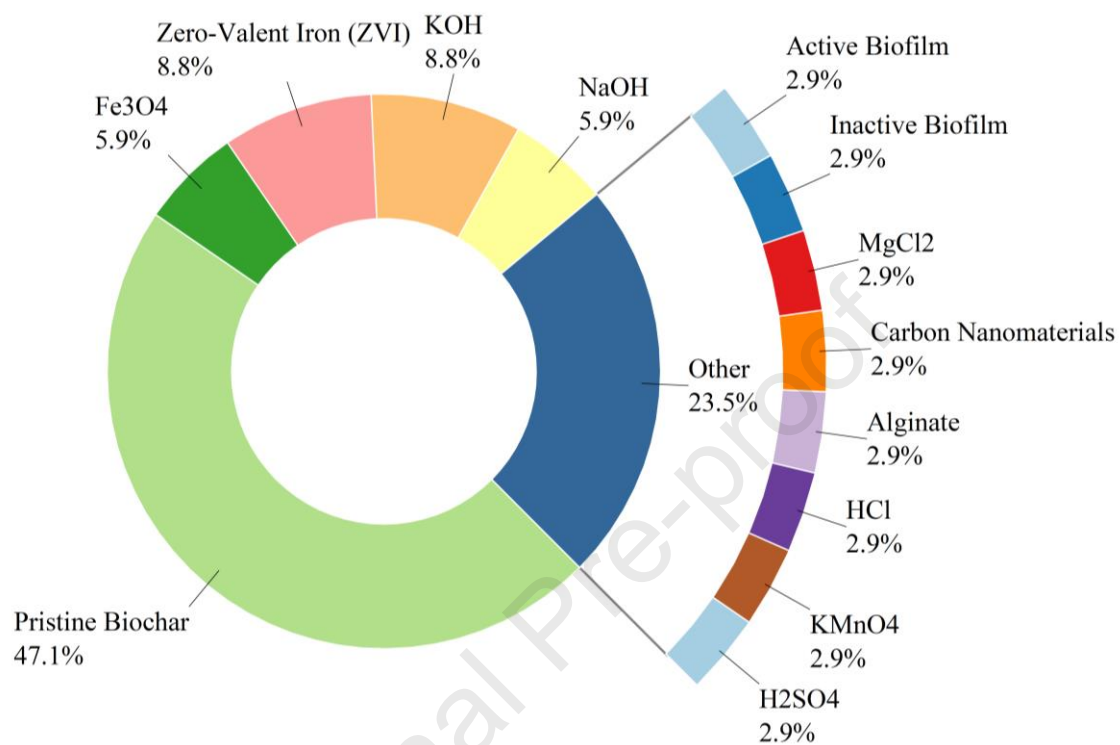


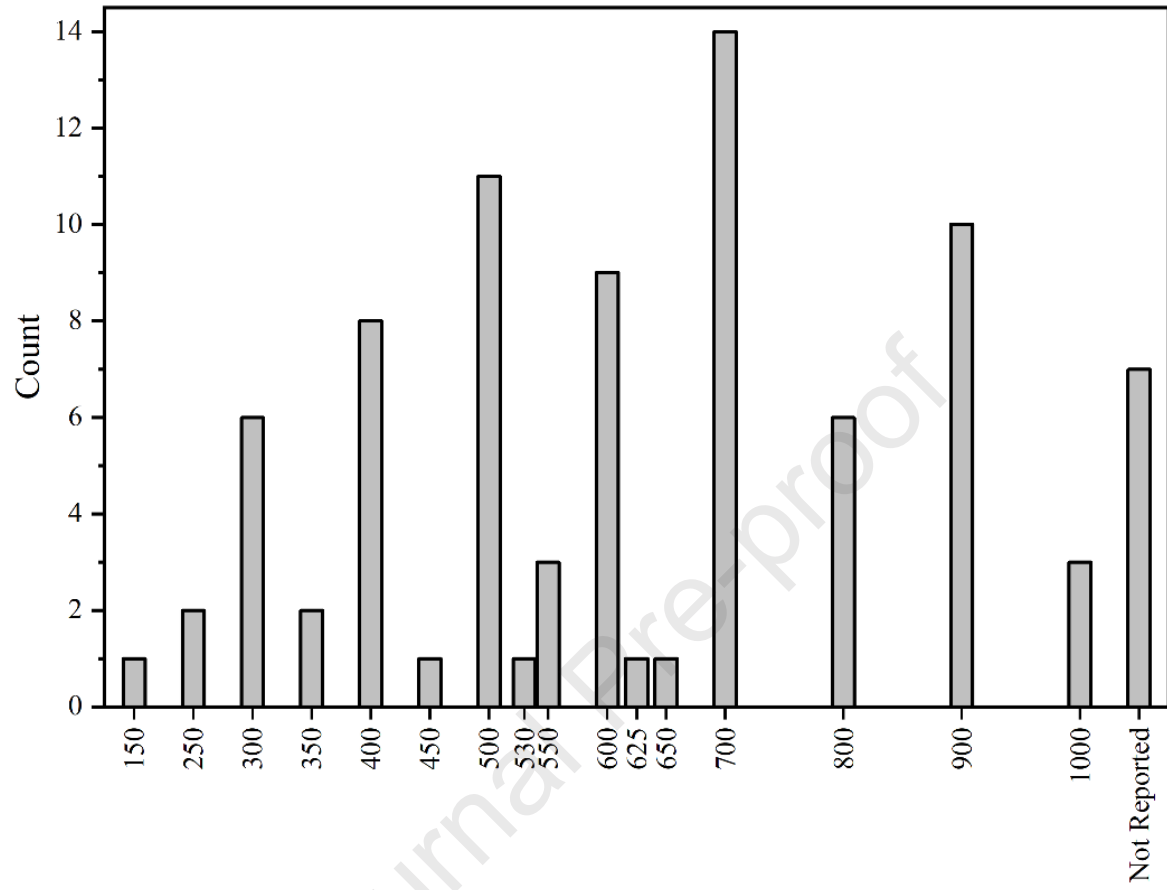


(a)



(b)





- Long-chain PFAS adsorb more effectively on biochar than short-chain PFAS.
- Functionalized biochar enhances PFAS removal via adsorption mechanisms.
- Pyrolysis temperature, pH, and PFAS chain length affect adsorption efficiency.

Journal Pre-proof